

# Periodic thermodynamics of isolated quantum systems

Achilleas Lazarides<sup>1</sup>, Arnab Das<sup>1,2</sup> and Roderich Moessner<sup>1</sup>

<sup>1</sup> Max-Planck-Institut für Physik komplexer Systeme, 01187 Dresden, Germany and

<sup>2</sup> Theoretical Physics Department, Indian Association for the Cultivation of Science, Kolkata 700032, India

(Dated: October 1, 2018)

The nature of the behaviour of an isolated many-body quantum system periodically driven in time has been an open question since the beginning of quantum mechanics [1–6]. After an initial transient, such a system is known to synchronize with the driving; in contrast to the non-driven case, no fundamental principle has been proposed for constructing the resulting non-equilibrium state. Here, we analytically show that, for a class of integrable systems, the relevant ensemble is constructed by maximizing an appropriately defined entropy subject to constraints [7] which we explicitly identify. This result constitutes a generalisation of the concepts of equilibrium statistical mechanics to a class of far-from-equilibrium-systems, up to now mainly accessible using ad-hoc methods.

There has recently been significant progress in our understanding of statistical mechanics based on the twin concepts of equilibration, the approach of a large, closed system's state to some steady state [1, 3, 4, 8–10, 12, 13], as well as of thermalization, when this steady state depends only upon a small number of quantities. Starting from ideas due to Jaynes [7], Srednicki and Deutsch [8, 9] and Popescu *et al* [16], both integrable and non-integrable closed, non-driven many-body systems have thus been shown to thermalize [4, 10, 12].

On the other hand, the study of periodically driven systems has also had a long history. Following early foundational work by Shirley [1] and Sambe [2], substantial theoretical and experimental progress has been made recently [3–6, 17–21].

Here, we combine ideas from the two areas to extend the concept of thermalization to the out-of-equilibrium case of periodically driven systems. By devising a mapping of the system to a set of effectively non-driven systems we show that a periodically driven system asymptotically approaches a time-periodic steady state at long times (see, e.g., [22] and our Suppl. Mat.). Specializing to a large class of integrable systems, we analytically show that Jaynes' entropy maximisation principle [7] gives a statistical mechanical description of the long-time, synchronized dynamics for infinite systems, and study the approach to this equilibrium state as a function of both the system size and time. Finally, we explain how our proposed setup is achievable with current experimental techniques.

Synchronization– The starting point for our analysis is the synchronization of the system with the driving, which may be seen as follows.

Consider a time-periodic Hamiltonian  $\hat{H}(t) = \hat{H}(t+T)$  and denote the time evolution operator over a period starting from time  $0 \leq \varepsilon < T$  by  $\hat{U}(\varepsilon, \varepsilon+T)$ . Taking  $\hbar = 1$ , we define an effective Hamiltonian  $\hat{H}_{\text{eff}}$  via

$$\exp[-i\hat{H}_{\text{eff}}T] = \hat{U}(0, T), \quad (1)$$

$\hat{H}_{\text{eff}}$  is a time-independent effective Hamiltonian which takes an initial state at  $t = 0$  to the same final state at  $t = T$  as the real time-dependent Hamiltonian  $\hat{H}(t)$ .

We concentrate on “stroboscopic” observations, that is,

observations at discrete points of time separated by a period,  $t_n = \varepsilon + nT$  for a given  $\varepsilon$ . The expectation value of an arbitrary time-independent operator  $\hat{\mathcal{O}}$  at time  $t$ ,  $\mathcal{O}(t) = \langle \psi(t) | \hat{\mathcal{O}} | \psi(t) \rangle$ , is

$$\mathcal{O}(t_n) = \langle \psi(0) | e^{i\hat{H}_{\text{eff}}nT} \hat{\mathcal{O}}^{(\varepsilon)} e^{-i\hat{H}_{\text{eff}}nT} | \psi(0) \rangle \quad (2)$$

where  $\hat{\mathcal{O}}^{(\varepsilon)} = \hat{U}^\dagger(0, \varepsilon) \hat{\mathcal{O}} \hat{U}(0, \varepsilon)$ . We have thus recast the time evolution into evolution under a time-independent Hamiltonian, at the price of introducing a set of new operators  $\hat{\mathcal{O}}^{(\varepsilon)}$ .

By analogy to a static quench [1, 3] (see Supplementary Material for a discussion of the necessary conditions), one can show that each series  $\{\mathcal{O}(t_n); n = 0, 1, 2, \dots\}$  converges to a fixed value. This immediately implies that the long-time behaviour of the system is periodic in time, i. e., synchronised.

Construction of the periodic ensemble– We now come to the main part of our work where we show that Jaynes' idea of entropy maximization [3, 7, 12] remains valid away from equilibrium for this class of models. In order to demonstrate that this is correct, we restrict ourselves to a class of tractable integrable Hamiltonians. For infinite systems, we show analytically that this ensemble correctly reproduces all correlation functions. For finite systems, we study the approach to the thermodynamic limit in a spatially inhomogeneous system of hard-core bosons (HCBs).

The Hamiltonians we consider are of the form

$$\hat{H}(t) = \sum_i \left[ \hat{a}_i^\dagger \mathcal{M}_{i,j}(t) \hat{a}_j + \hat{a}_i^\dagger \mathcal{N}_{i,j}(t) \hat{a}_j^\dagger + \text{h.c.} \right], \quad (3)$$

with the  $\hat{a}_i$  fermionic or bosonic operators,  $[a_i, a_j^\dagger]_{\pm} = \delta_{i,j}$ , and  $\mathcal{M}, \mathcal{N}$  are complex matrices. In cases of interest, the nonlinear, nonlocal transformation that brings the physical Hamiltonian to this form maps local observables to highly nonlocal, nonlinear functions of the  $\hat{a}$  operators.

For Hamiltonians bilinear in the operators  $\hat{a}$ ,  $\hat{H}_{\text{eff}}$  are bilinear and may therefore be brought to the form

$$\hat{H}_{\text{eff}} = \sum_{p=1}^L \omega_p \tilde{a}_p^\dagger \tilde{a}_p \quad (4)$$

by a unitary transformation ( $L$  is the system size). The operators  $\tilde{\mathcal{J}}_p(t) := \hat{U}(0, t) \tilde{a}_p^\dagger \tilde{a}_p \hat{U}^\dagger(0, t)$  (of which there are

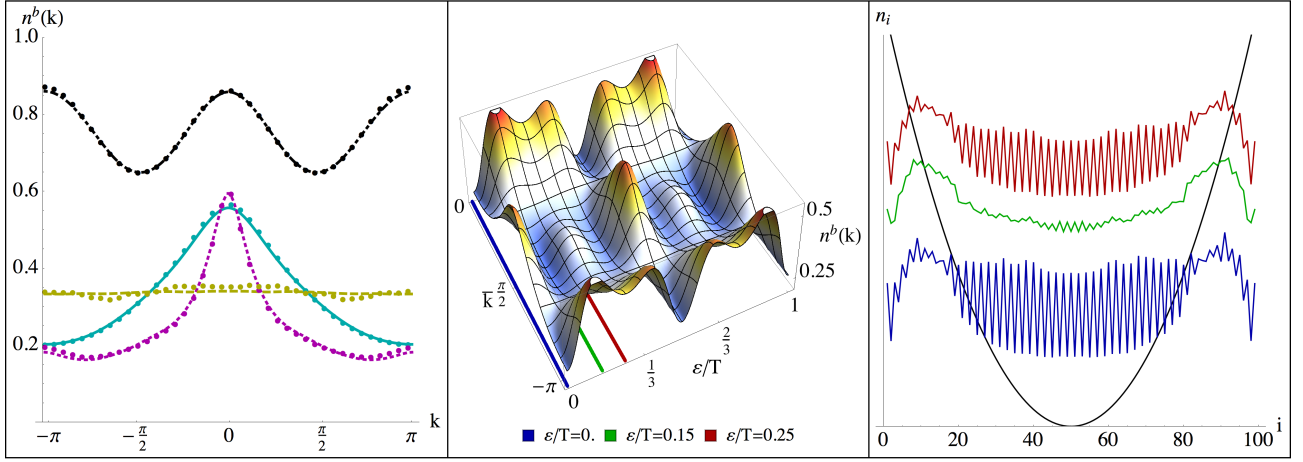


FIG. 1: Characterisation of the synchronised steady state. **Left:** Stroboscopic momentum distribution,  $\hat{n}(k) = L^{-1} \sum_{i,j} \hat{b}_i^\dagger \hat{b}_j \exp(-2\pi i k(i-j)L^{-1})$ , demonstrating the wide range of behaviour that occurs for varying parameters. The points correspond to snapshots of the dynamical evolution at late times ( $t = 490T$ ) for  $L = 200$ , while the continuous lines correspond to the PGE prediction. From top to bottom at the extreme left end of the plot, the amplitude of the superlattice potential, frequency and filling factor,  $(\Delta, \delta J, \omega, \nu)$  are  $(0.6, 0.5, 1.6, 3/4)$  (black, dot-dashed),  $(4, 0.5, 1.5, 1/3)$  (yellow, dashed),  $(4, 0.75, 2, 1/3)$  (cyan, full),  $(0.6, 0.5, 2, 1/4)$  (magenta, dotted) and  $\varepsilon = 0$ . The next two panels correspond to the parameters for the cyan full line. **Centre:** Expectation value of the momentum distribution  $\hat{n}(k)$  of the bosons during a single period in the synchronized state as a function of the time in the period,  $\varepsilon$ . The three lines on the time-momentum plane indicate the times  $\varepsilon/T = 0, 0.15, 0.25$  for which density distributions are shown in the rightmost panel. The momentum distribution undergoes qualitative changes: at some points of the period it has a single maximum at  $k = 0$  while at others it acquires double maxima at the edges of the Brillouin zone. **Right:** Each trace shows the expectation value of the density of the bosons,  $\hat{n}_i^b = \hat{b}_i^\dagger \hat{b}_i$ , at the time indicated in the middle panel by the line of the same colour, for a lattice size  $L = 100$  and offset for better visibility. The black line indicates the time average of the applied potential; the density peaks at the edges despite the potential being highest there, indicating a strongly non-equilibrium situation.

$L$ ) correspond to conserved quantities,  $\langle \psi(t) | \hat{\mathcal{S}}_p(t) | \psi(t) \rangle = \langle \psi(0) | \hat{\mathcal{S}}_p(0) | \psi(0) \rangle$  for all  $t$ , and are temporally periodic.

We now describe how to obtain the statistical ensemble describing the long-time behaviour of this system after a number of periods have elapsed. Given the set  $\{\hat{\mathcal{S}}_p(t)\}$  we construct the most general distribution maximizing Shannon's entropy in the space of periodic operators, subject to the constraints given by the conservation laws. The resulting ‘‘periodic Gibbs ensemble’’ (PGE) density operator is

$$\hat{\rho}_{PGE}(t) = \mathcal{Z}^{-1} \exp\left(-\sum_p \lambda_p \hat{\mathcal{S}}_p(t)\right) \quad (5)$$

with the  $\lambda_p$  fixed by requiring that  $\langle \psi(0) | \hat{\mathcal{S}}_p(0) | \psi(0) \rangle = \text{tr}(\hat{\rho}_{PGE}(0) \hat{\mathcal{S}}_p(0))$  and  $\mathcal{Z} = (\text{tr} \hat{\rho}_{PGE}(t))^{-1}$  a (time-independent) normalization factor.

Operator  $\hat{\rho}_{PGE}(t)$  has the following two properties: First, it correctly gives the conserved quantities:  $\text{tr}(\hat{a}_p^\dagger \hat{a}_q \hat{\rho}_{PGE}(t)) = \delta_{p,q} \langle \psi(t) | \hat{\mathcal{S}}_p(t) | \psi(t) \rangle$ . Secondly, since the  $\hat{\mathcal{S}}_p$  are periodic in time, it is itself manifestly periodic with time:  $\hat{\rho}_{PGE}(t) = \hat{\rho}_{PGE}(t+T)$ .

Finally we can analytically show that the PGE density matrix exactly reproduces all correlation functions in the thermodynamic limit; this somewhat lengthy but ultimately elementary calculation is described in the Supplementary Material. This constitutes our central conceptual result.

Application to Finite Systems: Numerical Results – Let

us now supplement the above exact and general results using numerical simulations for specific, finite systems. While the proof for the correctness of the PGE is strictly applicable only in the thermodynamic limit, we shall see that the deviation of finite systems from the PGE result rapidly decreases with system size.

A number of different physical systems may be mapped to Eq. (3) (see Supplementary Material). Here we present numerical results for the experimentally relevant case of HCBs subject to a simple potential, the Hamiltonian for which reads

$$\hat{H}_b(t) = -\frac{1}{2} \sum_i J_i(t) \hat{b}_i^\dagger \hat{b}_{i+1} + \text{h.c.} + \sum_i V_i(t) \hat{b}_i^\dagger \hat{b}_i \quad (6)$$

with the  $\hat{b}_i$  HCBs. The HCBs are described by operators  $\hat{b}$  obeying bosonic commutation relations,  $[\hat{b}_i, \hat{b}_j^\dagger] = \delta_{i,j}$ , with the additional hard-core condition  $\hat{b}_i^2 = 0$ . A Jordan-Wigner transformation,  $\hat{b}_i = \hat{a}_i \prod_{j<i} (-1)^{\hat{n}_j}$  with  $\hat{n}_j = \hat{b}_j^\dagger \hat{b}_j = \hat{a}_j^\dagger \hat{a}_j$ , maps  $\hat{H}_b(t)$  to Eq. (3) with  $\mathcal{M}_{i,j}(t) = -\frac{1}{2} J_i(t) (\delta_{i+1,j} + \delta_{i-1,j}) + \delta_{i,j} V_i(t)$ ,  $\mathcal{N}_{i,j} = 0$  and fermionic commutation relations for the  $\hat{a}$ .

Here we focus on a time-dependent superlattice potential superposed on a quadratic potential,  $V_i(t) = \frac{1}{2} ((i-L/2)/\ell_{ho})^2 + \Delta (-1)^i \cos(\omega t)$  and a time-dependent hopping amplitude  $J_i(t) = J + \delta J \cos(\omega t)$  with  $\omega = 2\pi/T$ . The protocol we use is to prepare the system in the

ground state in the presence of a harmonic potential  $V_i^{(0)} = \frac{1}{2}((i-L/2)/\ell_{ho})^2$ , fixing  $\ell_{ho} = N$ . This allows us to take the thermodynamic limit, since for large total number of particles the dimensionless parameter [28]  $\tilde{\rho} = N_b/\ell_{ho}$  plays a role analogous to the density in the uniform limit. Results with different system sizes but constant  $\tilde{\rho}$  are therefore comparable.

At time  $t = 0$ , the driving is switched on so that the total Hamiltonian is  $\hat{H}_b(t) = -\frac{1}{2}J\sum_i \hat{b}_i^\dagger \hat{b}_{i+1} + hc + \sum_i V_i(t)\hat{b}_i^\dagger \hat{b}_i$  with  $V_i(t) = V_i^{(0)} + \Delta(-1)^i \cos(2\pi t/T)$ .

Concentrating on the experimentally accessible momentum distribution of the bosons,  $\hat{n}^{(b)}(k) = L^{-1}\sum_{i,j} \hat{b}_i^\dagger \hat{b}_j \exp(-2\pi k(i-j)L^{-1})$  we use the numerical method used in, *inter alia*, [29]; it consists of solving the fermionic time-dependent problem and, at the end, inverting the Jordan-Wigner transformation.[30]

We begin by demonstrating a number of possible periodic states, corresponding to different parameters of the model. The leftmost panel of Figure 1 shows snapshots of the PGE momentum distribution  $\text{tr}(\hat{\rho}_{PGE}\hat{n}^{(b)}(k))$  at the beginning of each period ( $\varepsilon = 0$ ) for different parameter values. We emphasise that, away from the high-frequency regime, the corresponding time-averaged Hamiltonian [5, 23] is not an appropriate description. As a striking example, the black line shows a momentum distribution with peaks at the edges of the Brillouin zone. Concentrating now on the parameters corresponding to the cyan line, the central panel shows the time evolution of the momentum distribution over an entire period. Note, the system evolves through states in which the momentum is peaked at different locations of the Brillouin zone. Finally, the rightmost panel shows three snapshots of the density distribution of the same system at times indicated by the coloured lines in the central panel. The high spatial frequency oscillations and the peaking of the density at the edges is also very different from what would be obtained had the system been well-described by a time-averaged Hamiltonian, since the time-averaged potential (shown in black) is smooth and its potential highest at the edges.

We next discuss the approach to the long-time periodic state as a function of time and system sizes. After showing that the stroboscopic values of observables approach, then oscillate around, a constant value for each  $\varepsilon$ , we proceed to demonstrate that both this average value and the relative magnitude of the oscillations away from it decay to zero with increasing system size, in agreement with our analytical results for infinite systems. The approach is rapid: within a few periods, the system is practically thermalized.

The main plot of Fig. 2 shows the stroboscopic approach to the PGE state of the full bosonic momentum distribution,  $\hat{n}^{(b)}(k, mT)$ , for the parameters corresponding to the black line in Fig. 1. The entire momentum distribution approaches, then oscillates around, a period-independent result. The inset focusses on the component  $\hat{n}^{(b)}(k = \pi/2)$ , showing the stroboscopic time evolution of its difference from the value predicted by the PGE as a function of period, showing the oscillations about the equilibrium value shown by the heavy blue

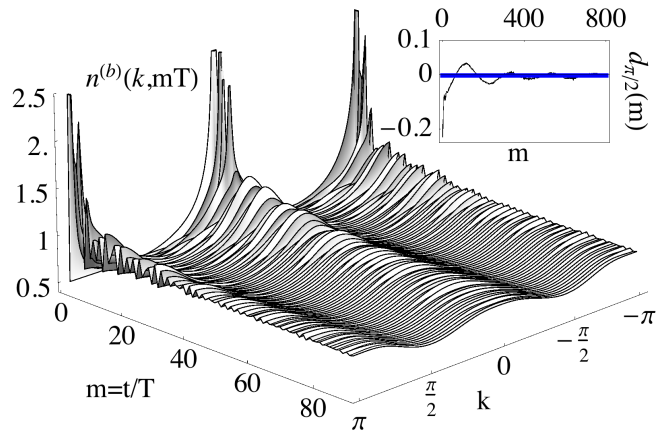


FIG. 2: **Main plot:** Stroboscopic approach to equilibrium with time for the full momentum distribution of the bosons,  $\hat{n}^{(b)}$ , corresponding to the heavy black line in Fig. 1 and for a system size  $L = 200$  sites. Note the brief initial transient period, followed by small oscillations around a well-defined limit. **Inset:** Same as the main plot, but for a single component of the momentum distribution. In this plot,  $d_{\pi/2}(m) = (\hat{n}^{(b)}(k = \pi/2, mT) - \hat{n}_{PGE}^{(b)}(k = \pi/2)) / \hat{n}_{PGE}^{(b)}(k = \pi/2)$  measures the deviation of the actual value from the prediction of the PGE. The heavy blue lines show the average of the deviations after discarding the first 50 periods, which approximates the long-time average. These plots demonstrate that the expectation value of the operator approaches, then oscillates about, a value that is very close (within a few percent) to the PGE prediction. Both the deviation of the average from the PGE prediction and the relative magnitude of the fluctuations about the mean value are shown to scale to zero with system size in Fig. 3.

lines.

We now quantitatively study the approach to the PGE limit as system size is increased. In Fig. 3 we plot the average of the distance of the dynamical momentum distribution from its PGE value over a number of periods,  $\bar{d} = (LN)^{-1} \sum_{m=n}^{n+N} \sum_k |\hat{n}^{(b)}(k, mT) - \hat{n}_{PGE}^{(b)}(k)|$ , as a function of the inverse system size  $1/L$ . These plots are for large  $n = 40L$  and  $N = 20L$  in order to allow plenty of time for equilibration. From Fig. 3, we conclude that the average of the momentum distribution approaches the PGE result, while fluctuations away from it average become smaller with increasing system size: as  $L \rightarrow \infty$ , the momentum distribution rapidly approaches the PGE periodic steady-state.

In conclusion, we have shown that the real dynamics rapidly approaches the thermodynamic-limit and long-time results for relatively small systems and short times.

**Experiments**—We now turn to the question of the experimental implementation of the specific system we have studied. To realize our proposal, three ingredients are required: A superlattice potential, periodic modulation and HCBs.

Experiments using a superlattice potential are already available [24], while periodic modulation of the lattice depth [17, 17, 25] is a standard technique. In particular, periodically driving a superlattice potential is described in Ref. [20]. Fi-

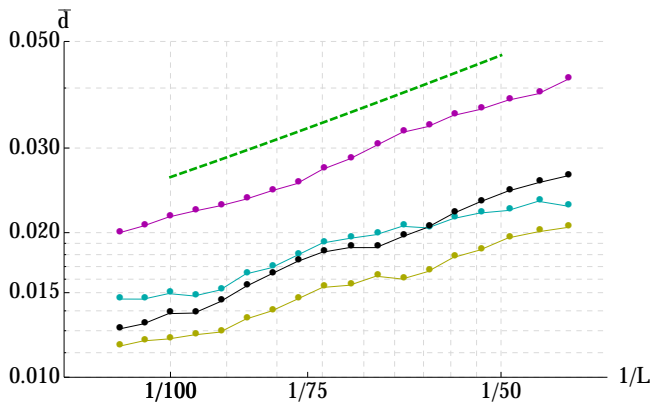


FIG. 3: (Color online) Approach to equilibrium with system size. The Hamiltonian and colour coding is the same as in Fig. 1. Here,  $\bar{d}$  measures distance from the PGE prediction,  $\bar{d} = (LN)^{-1} \sum_{m=n}^{n+N} \sum_k |\hat{n}(k, mT) - \hat{n}_{PGE}(k)|$ . We take  $n = 40L$  and  $N = 20L$ , large enough so that the results are insensitive to further increase. The dashed green line is a plot of  $\bar{d} \propto L^{-1}$  to guide the eye. These results strongly suggest that the distance of the long-time behaviour of the system from our prediction at the thermodynamic limit falls off as a power law.

nally, the HCB regime may be achieved via confinement-induced resonance, which involves manipulating the radial harmonic potential strength [26, 27].

The example we have studied above is therefore accessible with current experimental techniques.

**Conclusions and outlook**—For a large class of integrable periodically-driven systems, we have shown that a periodic steady-state is attained at long times. To describe this state, we have constructed a periodic version of the generalized Gibbs ensemble (GGE) [12], commonly introduced in connection with quenches in integrable models. We have provided an analytical demonstration that it exactly reproduces the periodic steady-state in the thermodynamic limit. We also provide numerical evidence of rapid convergence (i) to the thermodynamic-limit prediction with increasing system size and (ii) to the steady-state with time.

It would be natural to extend our results to a generic non-integrable situation. Our PGE is analogous to the GGE for non-driven systems [12]; the analogy would suggest that, for a closed, non-integrable, periodically-driven system, a subsystem for which the rest of the system plays the role of a bath might be described by the periodic density matrix operator  $\exp(\hat{H}_{\text{eff}}(\varepsilon) = \hat{U}(0, \varepsilon) \hat{H}_{\text{eff}} \hat{U}^\dagger(0, \varepsilon))$ , analogous to the Gibbs ensemble for non-driven systems [16]. Unfortunately, there are several issues with this; chief amongst them are that  $\hat{H}_{\text{eff}}(\varepsilon)$  is not a local operator in general and, more seriously, that  $\hat{H}_{\text{eff}}(\varepsilon)$  is not uniquely defined (its eigenvalues are only defined modulo  $2\pi/T$ —we do not use the eigenvalues and therefore circumvent this problem in our work). We are currently investigating possible resolutions of these conceptual issues.

Our work here should be compared to the usual situation for

out-of-equilibrium systems, where each case has to be studied individually using ad-hoc techniques tailored to the specific problem at hand. In contrast, for this type of periodically-driven systems the general framework of maximum entropy statistical mechanics applies as-is. It not only gives the correct ensemble but also allows detailed computation of physical observables. We hope that this work will motivate the search for further such “thermodynamic” principles governing driven systems in all generality.

## ACKNOWLEDGMENTS

We acknowledge discussions with M. Aidelsburger, M. Atala and J. T. Barreiro. A. L. thanks M. Kollar, O. Tieleman, P. Ribeiro, A. Eckardt, T. Scheler, A. Sen, V. Bastidas, and M. Haque for discussions. AD acknowledges inspiring general discussions with E. Tosatti on non-equilibrium in the past.

- 
- [1] J. H. Shirley, Phys. Rev. **138**, B979 (1965).
  - [2] H. Sambe, Phys. Rev. A **7**, 2203 (1973).
  - [3] M. Grifoni and P. Hanggi, Physics Reports **304**, 229 (1998).
  - [4] A. Das, Phys. Rev. B **82**, 172402 (2010).
  - [5] A. Eckardt, C. Weiss, and M. Holthaus, Phys. Rev. Lett. **95**, 260404 (2005).
  - [6] N. H. Lindner, G. Refael, and V. Galitski, Nature Physics **7**, 490 (2011).
  - [7] E. T. Jaynes, Phys. Rev. **106**, 620 (1957).
  - [8] M. Srednicki, Physical Review E **50**, 888 (1994).
  - [9] J. M. Deutsch, Phys. Rev. A **43**, 2046 (1991).
  - [10] M. Rigol, V. Dunjko, and M. Olshanii, Nature **452**, 854 (2008).
  - [11] M. A. Cazalilla, A. Iucci, and M.-C. Chung, Phys. Rev. E **2012**, 011133 (2012).
  - [12] M. Rigol, V. Dunjko, V. Yurovsky, and M. Olshanii, Phys. Rev. Lett. **98**, 050405 (2007).
  - [13] P. Calabrese, F. H. L. Essler, and M. Fagotti, Phys. Rev. Lett. **106**, 227203 (2011).
  - [14] P. Reimann, Phys. Rev. Lett. **101**, 190403 (2008).
  - [15] M. Fagotti and F. H. L. Essler, Phys. Rev. B **87**, 245107 (2013).
  - [16] S. Popescu, A. J. Short, and A. Winter, Nature Physics **2**, 754 (2006).
  - [17] T. Stöferle, H. Moritz, C. Schori, M. Köhl, and T. Esslinger, Phys. Rev. Letters **92**, 130403 (2004).
  - [18] H. Lignier, A. Zenesini, D. Ciampini, O. Morsch, E. Arimondo, S. Montangero, G. Pupillo, and R. Fazio, Phys. Rev. A **79**, 041601 (2009).
  - [19] E. Haller, M. Gustavsson, M. J. Mark, J. G. Danzl, R. Hart, G. Pupillo, and H.-C. Naegerl, Science **325**, 1224 (2009).
  - [20] T. Iadecola, C. Chamon, R. Jackiw and S.-Y. Pi, Phys. Rev. B **88**, 104302 (2013).
  - [21] Y.-A. Chen, S. Nascimbène, M. Aidelsburger, M. Atala, S. Trotzky, and I. Bloch, Phys. Rev. Lett. **107**, 210405 (2011).
  - [22] A. Russomanno, A. Silva, and E. Santoro, Phys. Rev. Lett. **109**, 257201 (2012).
  - [23] A. Eckardt, M. Holthaus, H. Lignier, A. Zenesini, D. Ciampini, O. Morsch, and E. Arimondo, Phys. Rev. A **79**, 013611 (2009).

- [24] M. Atala, M. Aidelsburger, J. T. Barreiro, D. Abanin, T. Kitagawa, E. Demler, and I. Bloch, *Nature Physics* **9**, 795 (2013).
- [25] E. Haller, R. Hart, M. J. Mark, J. G. Danzl, L. Reichsöllner, M. Gustavsson, M. Dalmonte, G. Pupillo, and H. C. Nägerl, *Nature* **466**, 597 (2010).
- [26] M. Olshanii, *Phys. Rev. Lett.* **81**, 938 (1998).
- [27] E. Haller, M. J. Mark, R. Hart, J. G. Danzl, L. Reichsöllner, V. Melezhik, P. Schmelcher, and H. C. Nägerl, *Phys. Rev. Lett.* **104**, 153203 (2010).
- [28] M. Rigol and A. Muramatsu, *Phys. Rev. A* **70**, 031603 (2004).
- [29] M. Rigol and A. Muramatsu, *Mod. Phys. Lett. B* **19**, 861 (2005).
- [30] It is worth pointing out that  $\hat{n}^{(b)}$  for the bosons is neither bilinear nor local in terms of the Jordan-Wigner fermions, since  $\hat{b}_i^\dagger \hat{b}_j = \hat{a}_i^\dagger \left( \prod_{i \leq m < j} (-1)^{\hat{n}_m} \right) \hat{a}_j$ . We therefore expect the PGE predictions to only approximate the real dynamics, becoming exact at the thermodynamic limit.

## SYNCHRONIZATION

We first show how a periodically driven system synchronizes with the driving. This is analogous to the way a non-driven system equilibrates [1, 2], with most observables approaching a time-independent steady-state in which contributions from off-diagonal (in the energy basis) matrix elements are negligible. This is usually called the ‘‘diagonal ensemble’’ (DE).

Consider the expectation value of the operator  $\hat{\mathcal{O}}$  at time  $t_n = \varepsilon + nT$ ,  $\mathcal{O}(t_n) = \text{tr}(\rho(t_n)\hat{\mathcal{O}})$ . Introducing the rotated operator defined in the main text,

$$\mathcal{O}(t_n) = \text{tr}\left(e^{-i\hat{H}_{\text{eff}}nT}\hat{\rho}(0)e^{i\hat{H}_{\text{eff}}nT}\hat{\mathcal{O}}^{(\varepsilon)}\right)$$

can be viewed as the expectation value of the rotated operator  $\hat{\mathcal{O}}^{(\varepsilon)}$  evolving under a time-independent Hamiltonian  $\hat{H}_{\text{eff}}$  at time  $nT$  starting from the initial state  $\hat{\rho}(0)$ . For such a static quench, and under a set of general assumptions for the initial state [1–3], one expects each series  $\{\mathcal{O}(nT + \varepsilon); n = 0, 1, 2, \dots\}$  to converge to a fixed value [16]. Denote the eigenvalues and eigenstates of  $\hat{H}_{\text{eff}}$  by  $\varepsilon_\alpha$  and  $|\alpha\rangle$ , respectively, with  $\alpha = 1 \dots D_{\mathcal{H}}$  and  $D_{\mathcal{H}}$  the dimension of the Hilbert space of the system. Expanding  $\hat{\rho}(0) = \sum_{\alpha,\beta} \rho_{\alpha,\beta} |\alpha\rangle\langle\beta|$ , the limit of the long-time average over many periods is given by

$$\lim_{N \rightarrow \infty} N^{-1} \sum_{n=1}^N \mathcal{O}(nT + \varepsilon) = \sum_{\alpha=1}^{D_{\mathcal{H}}} \rho_{\alpha,\alpha} \langle\alpha|\hat{\mathcal{O}}^{(\varepsilon)}|\alpha\rangle, \quad (7)$$

analogously to the DE result for a static system.

It has been shown by Reimann [1] that there are two necessary conditions for the equality (7) to be accurate. Firstly, defining the inverse participation ratio in the eigenstate basis by

$$\phi_q = \sum_{\alpha} |c_\alpha|^{2q} \quad (8)$$

it is necessary that  $\phi_2 \ll 1$ , that is, a sufficiently large fraction of the eigenstates of  $\hat{H}_{\text{eff}}$  must be occupied. Secondly, the range of possible eigenstate expectation values of the operator in question,  $\hat{\mathcal{A}} = \hat{\mathcal{O}}^{(\varepsilon)}$ , must be finite, ie,  $\Delta_{\mathcal{A}} = \max_{\psi} \langle\psi|\hat{\mathcal{A}}|\psi\rangle - \min_{\psi} \langle\psi|\hat{\mathcal{A}}|\psi\rangle$  must be finite. If these two conditions hold, then a modification of the arguments of Ref. [1, 2] shows that the mean square deviation of the actual time evolution from the prediction of the diagonal ensemble,

$$\sigma_{\mathcal{A}}^2 = \overline{(\mathcal{O}(nT + \varepsilon) - \text{tr}(\hat{\mathcal{O}}\hat{\rho}_{PGE}(\varepsilon)))^2} \quad (9)$$

where  $\overline{f(n)} = \lim_{N \rightarrow \infty} N^{-1} \sum_{n=1}^N f(n)$  is bounded by

$$\sigma_{\mathcal{A}}^2 \leq \Delta_{\mathcal{A}} \phi_2. \quad (10)$$

All observables we consider (such as the single-particle momentum distribution) clearly have a finite  $\Delta_{\mathcal{A}}$ , so that we conclude that synchronization occurs for any initial state sufficiently nonlocal in the basis formed by the eigenstates of  $\hat{H}_{\text{eff}}$ .

## PROOF THAT THE PGE CAPTURES THE SYNCHRONIZED STATE

We now turn to the special case of integrable systems that can be mapped to the form of Eq. (3) of the main text (possibly via a Jordan-Wigner transformation). For simplicity, we also specialise to pure initial states, such that  $\hat{\rho}(0) = |\psi(0)\rangle\langle\psi(0)|$  and  $\rho_{\alpha,\beta} = c_\alpha^* c_\beta$  with  $c_\alpha = \langle\psi(0)|\alpha\rangle$ . Our goal is to show that the expectation value of any operator  $\hat{\mathcal{O}}$  at any time  $\varepsilon$  in the long-time limit is equal to  $\text{tr}(\hat{\mathcal{O}}\hat{\rho}_{PGE}(\varepsilon))$ .

In this section, the operators  $\hat{a}$  refer to the operators diagonalising  $\hat{H}_{\text{eff}}$  (they are defined in Eq. 4 of the main text), while the states denoted by Greek letters such as  $|\alpha\rangle$  refer to the many-body eigenstates of  $\hat{H}_{\text{eff}}$ , as in the previous section.

Let us begin by considering bilinear operations  $\hat{\mathcal{O}}$ . Writing  $\hat{\mathcal{A}} = \hat{\mathcal{O}}^{(\varepsilon)}$ , defining the long-time limit (see Eq. (7))  $\mathcal{A}_L = \sum_{\alpha=1}^{D_{\mathcal{H}}} |c_\alpha|^2 \langle\alpha|\hat{\mathcal{A}}|\alpha\rangle$  and expanding  $\hat{\mathcal{A}}$  in the  $\tilde{a}_p$ ,  $\hat{\mathcal{A}} = \sum_{p,q} (\mathcal{A}_{p,q} \tilde{a}_p^\dagger \tilde{a}_q + \mathcal{B}_{p,q} \tilde{a}_p \tilde{a}_q + \mathcal{C}_{p,q} \tilde{a}_p^\dagger \tilde{a}_q^\dagger)$ , we have

$$\mathcal{A}_L = \sum_{\alpha,p,q} \mathcal{A}_{p,q} |c_\alpha|^2 \langle\alpha|\tilde{a}_p^\dagger \tilde{a}_q|\alpha\rangle. \quad (11)$$

We now use the identities  $\langle\alpha|\tilde{a}_p^\dagger \tilde{a}_q|\alpha\rangle = \langle\alpha|\tilde{a}_p^\dagger \tilde{a}_q|\alpha\rangle \delta_{p,q}$  and  $\langle\alpha|\tilde{a}_p^\dagger \tilde{a}_q|\beta\rangle \delta_{p,q} = \langle\alpha|\tilde{a}_p^\dagger \tilde{a}_q|\alpha\rangle \delta_{p,q} \delta_{\alpha,\beta}$ , the second of which follows from  $[\hat{H}_{\text{eff}}, \hat{N}] = 0$  with  $\hat{N}$  the particle number operator, finally arriving at

$$\mathcal{A}_L = \sum_p \mathcal{A}_{p,p} \mathcal{I} p(0) \quad (12)$$

with  $\mathcal{I} p(0) = \langle\psi(0)|\hat{\mathcal{I}}_p(0)|\psi(0)\rangle = \langle\psi(0)|\tilde{a}_p^\dagger \tilde{a}_p|\psi(0)\rangle$ . Therefore,

$$\mathcal{A}_L = \sum_{p=1}^L \mathcal{A}_{pp} \langle\psi(0)|\hat{\mathcal{I}}_p(0)|\psi(0)\rangle. \quad (13)$$

Explicit calculation then shows that  $\text{tr}(\hat{\mathcal{O}}\hat{\rho}_{PGE}(\varepsilon)) = \text{tr}(\hat{\mathcal{A}}\hat{\rho}_{PGE}(0)) = \mathcal{A}_L$ . Thus, the long-time limit for the expectation of any bilinear operator  $\hat{\mathcal{A}}$  is exactly reproduced by the PGE density matrix for any time  $\varepsilon \in [0, T)$ .

Using Wick’s theorem we can extend this result to higher-order (than bilinear) operators, at least in the absence of accidental symmetries [4, 5] and in the thermodynamic limit (both conditions are necessary in order for fluctuations to vanish and Wick’s theorem to be applicable).

Consider an arbitrary higher-order operator  $\hat{\mathcal{O}}$ , involving terms with more than two fermionic operators (it is always possible to express any  $\hat{\mathcal{O}}$  as a sum of products of fermionic operators).

We now take an initial state that is an eigenstate of some bilinear Hamiltonian without translational invariance [17]. As the time evolution occurs under another quadratic Hamiltonian, the expectation value of each product of fermionic operators factorises at each instant in time according to Wick’s theorem [6, Sec. 14]. For example, for an  $M$ -particle operator,  $\hat{\mathcal{A}} =$

$\tilde{a}_{p_1}^\dagger \cdots \tilde{a}_{p_M}^\dagger \tilde{a}_{p_1} \cdots \tilde{a}_{p_M}$ , defining  $\langle \cdots \rangle(t) = \text{tr}(\cdots \hat{\rho}(t))$  we have  $\langle \hat{\mathcal{O}} \rangle(t) = \sum_{\mathcal{P}} (-1)^{|\mathcal{P}|} \langle \tilde{a}_{p_{\mathcal{P}_1}}^\dagger \tilde{a}_{p_{\mathcal{P}_1}} \rangle(t) \cdots \langle \tilde{a}_{p_{\mathcal{P}_M}}^\dagger \tilde{a}_{p_{\mathcal{P}_M}} \rangle(t)$  where  $\mathcal{P}$  denotes a permutation. If the long-time limit  $\lim_{t \rightarrow \infty} \langle \tilde{a}_j^\dagger \tilde{a}_q \rangle(t)$  exists, then, by the earlier argument for bilinear operators, it is given by the PGE result and therefore  $\lim_{N \rightarrow \infty} N^{-1} \sum_{n=0}^N \langle \hat{\mathcal{O}} \rangle(nT + \varepsilon) = \text{tr} \langle \hat{\rho}_{PGE}(\varepsilon) \rangle$  even for the higher-order correlators. If, on the other hand, the limit does not exist then the proof fails and higher-order operators are not guaranteed to be reproduced by the PGE. For infinite systems,  $\langle \tilde{a}_j^\dagger \tilde{a}_q \rangle(t)$  generally approaches a limit for  $t \rightarrow \infty$ .

In conclusion, the main assumption necessary for this result is that the expectation values of bilinear operators tend to a well-defined limit at long times; this is generally true for systems in the thermodynamic limit [1, 2]. However, even in the thermodynamic limit it is known to fail for disordered systems [7, 8].

### EXAMPLE HAMILTONIANS

In the main text we concentrate on a system of hard-core bosons. Here, we explicitly list a number of other important physical Hamiltonians that may be mapped to the form

$$\hat{H}(t) = \sum_i \left[ \hat{a}_i^\dagger \mathcal{M}_{i,j}(t) \hat{a}_j + \hat{a}_i^\dagger \mathcal{N}_{i,j}(t) \hat{a}_j^\dagger + \text{h.c.} \right], \quad (14)$$

with  $\hat{a}$  either bosonic or fermionic.

**Luttinger Liquids:** Another important class of Hamiltonians with broad applications is given by Eq. (3) with the  $\hat{a}$  satisfying bosonic commutation relations. In particular, Luttinger liquids (LLs) [9, 10] are in the class of one-dimensional systems described by such a Hamiltonian. As a concrete example, the Hamiltonian for a spatially homogeneous time-dependent LL may be written in the form [5, 11, 12]

$$\hat{H} = \sum_{q \neq 0} \left( \omega(q, t) \hat{b}_q^\dagger \hat{b}_q + \frac{1}{2} g(q, t) \left[ \hat{b}_q \hat{b}_{-q} + \hat{b}_q^\dagger \hat{b}_{-q}^\dagger \right] \right) \quad (15)$$

with  $\hat{b}_q$  bosonic operators and  $\omega(q, t)$  and  $g(q, t)$  periodically time-dependent coefficients [18].

**XY Chain:** Another very well-studied model Hamiltonian is the spin-1/2 quantum XY chain, for which  $\hat{H}_{XY}(t) = \sum_i [J_x(t) \hat{\sigma}_i^x \hat{\sigma}_{i+1}^x + J_y(t) \hat{\sigma}_i^y \hat{\sigma}_{i+1}^y + B(t) \hat{\sigma}_i^z]$  with the  $\hat{\sigma}$  spin-1/2 operators. Using again a standard Jordan-Wigner transformation [13], this is mapped to Eq. (3) with  $\mathcal{M}_{i,j}(t) = (J_x(t) + J_y(t)) (\delta_{i,i+1} + \delta_{i,i-1}) + B(t) \delta_{i,j}$  and  $\mathcal{N}_{i,j}(t) = (J_x(t) - J_y(t)) (\delta_{i,i+1} + \delta_{i,i-1})$ .

- [5] B. Dóra, A. Bácsi, and G. Zaránd, Phys. Rev. B **86**, 161109 (2012).
- [6] L. D. Landau and E. M. Lifshitz, Statistical Physics, Vol. 2 (Pergamon Press, Oxford, 1980).
- [7] S. Ziraldo, A. Silva, and G. E. Santoro, Phys. Rev. Lett. **109**, 247205 (2012).
- [8] S. Ziraldo and G. E. Santoro, Phys. Rev. B **87**, 064201 (2013).
- [9] F. D. M. Haldane, Phys. Rev. Lett. **47**, 1840 (1981).
- [10] T. Giamarchi, Quantum Physics in One Dimension (Clarendon Press, Oxford, 2003).
- [11] M. A. Cazalilla, J. Phys. B **37**, S1 (2004).
- [12] B. Dora, M. Haque, and G. Zaránd, Phys. Rev. Lett. **106**, 156406 (2011).
- [13] X.-G. Wen, Quantum Field Theory of Many-Body Systems (Oxford University Press, Oxford, 2004).
- [14] D. M. Gangardt and G. V. Shlyapnikov, Phys. Rev. Lett. **90** (2003).
- [15] A. Lazarides, O. Tieleman, and C. Morais Smith, Phys. Rev. A **84**, 023620 (2011).
- [16] To be more precise, for a finite system, successive elements of  $\{\hat{\mathcal{O}}(nT + \varepsilon; n = 0, 1, 2, \dots)\}$  will approach and then oscillate around a time-independent value.
- [17] Translational invariance introduces “accidental” correlations in the initial state [4, 5]
- [18] Physically, a LL is usually obtained as an approximate hydrodynamic description of, for example, a strongly-interacting bosonic system in one dimension [9–11, 14, 15], and is not expected to correctly describe highly excited states of the physical system. The question of whether the dynamics of a given periodically-driven system is correctly described by a driven LL therefore requires a detailed case-by-case analysis. Here, we consider a periodically-driven LL as a model system without discussing its applicability to specific experimental situations.

- 
- [1] P. Reimann, Phys. Rev. Lett. **101**, 190403 (2008).
  - [2] P. Reimann and M. Kastner, New. J. Phys. **14**, 043020 (2012).
  - [3] M. A. Cazalilla, A. Iucci, and M.-C. Chung, Phys. Rev. E **2012**, 011133 (2012).
  - [4] M. Fagotti and F. H. L. Essler, Phys. Rev. B **87**, 245107 (2013).